

CHAPTER 2

EXPERIMENTAL

2.1 Introduction

This experiment uses a temperature-controlled flash kinetic spectrometer to measure the rate of the following chain reaction:



The rate constant is measured by monitoring the time-dependant OH radical concentration via direct infrared absorption. The infrared source is an F-center laser, tuned to the $v=1 \leftarrow 0$ $P(5/2)_1^-$ transition of OH radical, which probes the most populated state at room temperature. The P branch is chosen over the R branch because the Einstein A coefficient is slightly larger¹. In order to simplify the kinetics, $[\text{O}_3]$ is at least 1000 times greater than $[\text{OH}]$, which results in pseudo-first order behavior.

2.2 The Experimental Apparatus

The apparatus used in this experiment is the temperature-controlled flash kinetic spectrometer shown in figure 2-1.^{2,3} The spectrometer consists of a temperature-controlled flow tube into which various precursor and reactive gases are introduced.

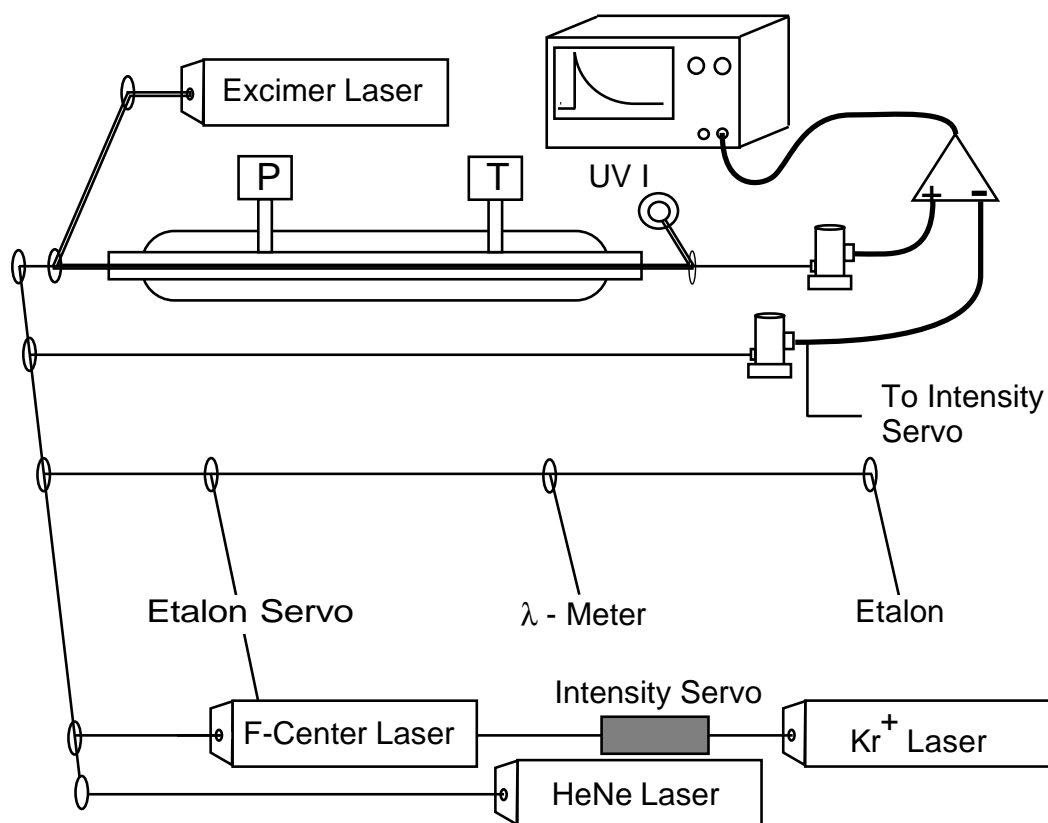


Figure 2-1. Experimental setup. $O(^1D)$ is created by photolysis of O_3 at 308 nm. The $O(^1D)$ reacts quickly with H_2O and H_2 to form OH . The time-dependent OH concentration is then probed by the F-center laser tuned to the $v=1 \leftarrow 0 P(5/2)1^-$ transition. The infrared light is detected by liquid-nitrogen cooled InSb detectors. Signal subtraction and the intensity servo serve to reduce common-mode noise.

The reaction scheme, shown in figure 2-2, is initiated by a 10 ns pulse from a XeCl excimer laser (308 nm). The UV light serves to photolyze 1% of the ozone

present in the excimer beam, based on a beam diameter of 1 cm, a pulse energy of 0.5 mJ/pulse, and a 308 nm ozone cross section of $1.35 \times 10^{-19} \text{ cm}^2$. At room temperature⁴, the branching ratio for the $\text{O}(^1\text{D})$ product from the ozone photolysis is 80%. Following the photolysis, the $\text{O}(^1\text{D})$ is free to react with precursor gases (H_2 and H_2O).

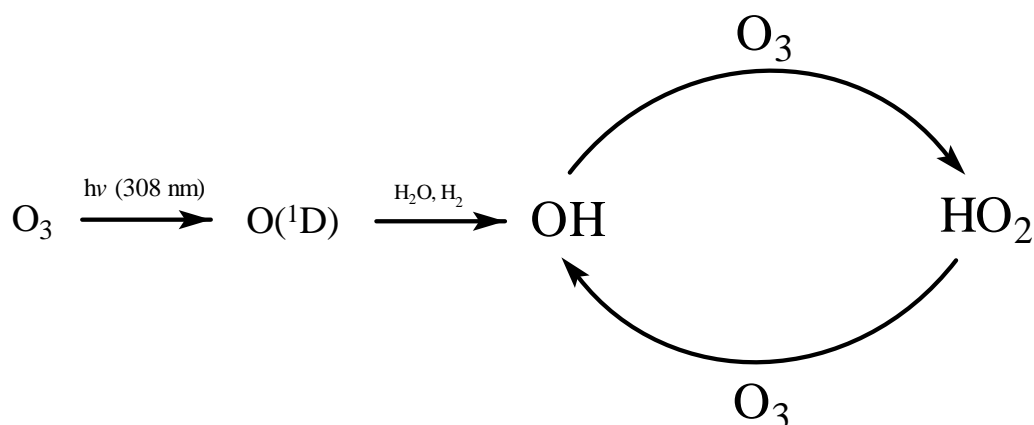


Figure 2-2. Reaction scheme of the OH/HO₂/O₃ chain reaction. An excimer laser tuned to 308 nm photolyzes approximately 1% of the ozone in the 1cm diameter excimer beam. The resulting $\text{O}(^1\text{D})$ then reacts with H_2O and H_2 to form OH radical ($k_{\text{H}_2\text{O}} = 2.2 \times 10^{-10} \text{ cm}^3/\text{sec}$, $k_{\text{H}_2} = 1.0 \times 10^{-10} \text{ cm}^3/\text{sec}$). In addition, the H_2O in the cell serves to vibrationally cool the OH into its ground state ($k_{\text{relax}} = 1.4 \times 10^{-11} \text{ cm}^3/\text{sec}$). The ground state OH is probed via direct infrared absorption while it undergoes the chain reaction.

In addition to being an OH precursor, the H_2O serves to vibrationally cool any excited OH into its ground state.



The concentration of radicals in the flow tube is a linear function of excimer laser pulse energy and ozone concentration. In an effort to keep probability of radical-based side reactions to a minimum, the excimer pulse energy is kept as low as possible (~0.5 mJ/pulse), yielding a typical OH radical concentration of 1×10^{12} molecules/cm³. Even assuming gas-kinetic rates for radical-radical reactions, the time scale for these reactions is on the order of 10 msec, which is at least an order of magnitude slower than the reaction of OH with ozone.

The temporal profile of the OH radical concentration is probed via an F-center laser, which is capable of continuous, single-mode operation⁵ between 2.5 and 3.3 μm (4000 and 3030 cm^{-1}), with a linewidth of 2 MHz. In order to measure the frequency of the IR light, a portion of it is sent to a λ -meter (traveling Michelson interferometer) built after the design by Hall and Lee⁶, using a polarization stabilized HeNe laser as a reference.

The temperature-controlled flow cell consists of an inner 106 cm long, 1" diameter quartz tube surrounded by a 3" diameter quartz jacket as shown in figure 2-3.

The temperature of the gas within the tube is maintained by pumping fluid between a heat-transfer coil and the outer jacket of the cell. Our current pumping system exchanges the fluid in the outer jacket every 15 seconds. Temperature within the cell is measured via a K type thermocouples (Chromel-Alumel) located just above the probe region of the inner tube. By using a transverse flow across the tube, temperature gradients are kept to a minimum (0.5(5)^o C).

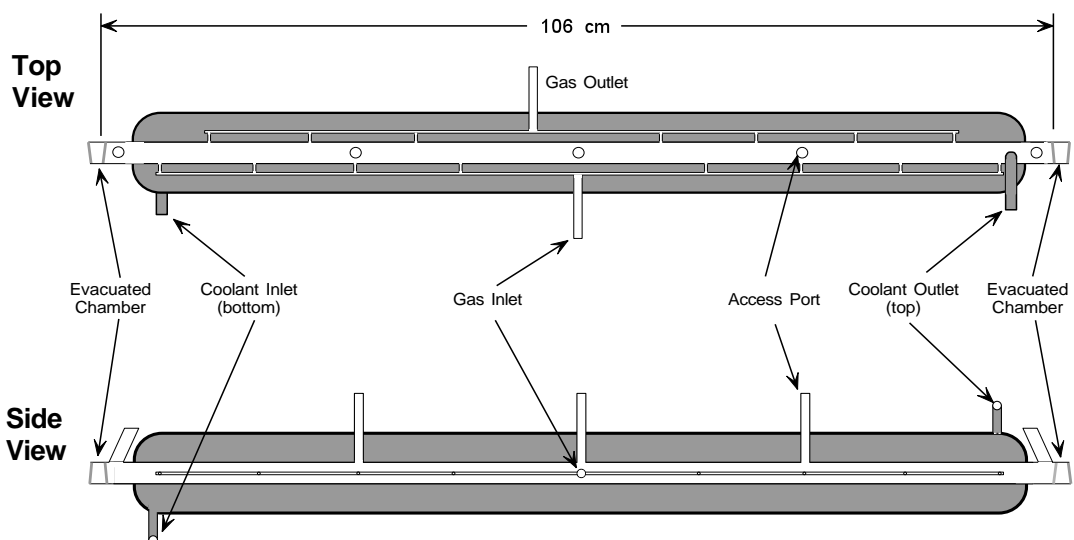


Figure 2-3. The temperature-controlled flow cell. The above figure shows the layout of the temperature-controlled flow cell. The gas inlet and outlet manifolds are designed such that gas flows across the cell (transverse flow). Transverse flow serves to reduce temperature and concentration gradients along the length of the cell. Surrounding the reaction chamber is a cooling jacket through which a temperature-controlled fluid is pumped. Also shown is the various access ports where we measure temperature and pressure of the gas.

Prior to entering the cell, the IR laser beam is split into two beams, which serve as signal and reference. The IR signal and excimer beams are overlapped via a 90% IR transmissive, 95% UV reflective dichroic mirror, and sent down the middle of the flow tube. The reference beam travels directly to the detector. The signal and reference beams are detected via 0.25 mm diameter, cryogenically-cooled InSb detectors. The detectors operate with a transimpedance of 50 k Ω and a bandwidth of 1 MHz. The resulting signals from the detector/amplifier combination are then sent to a differential amplifier, which allows subtraction of the common-mode noise. In addition, the reference signal is sent to an intensity stabilization servo, developed by Bill Chapman and Terry Brown⁷. This servo uses an electro-

optic (EO) modulator to vary the intensity of the Kr ion pump laser in an effort to cancel the noise on the reference detector. The combination of the intensity modulation servo and signal subtraction results in noise figures that are within a factor of 2 of the shot-noise limit, as shown in figure 2-4.

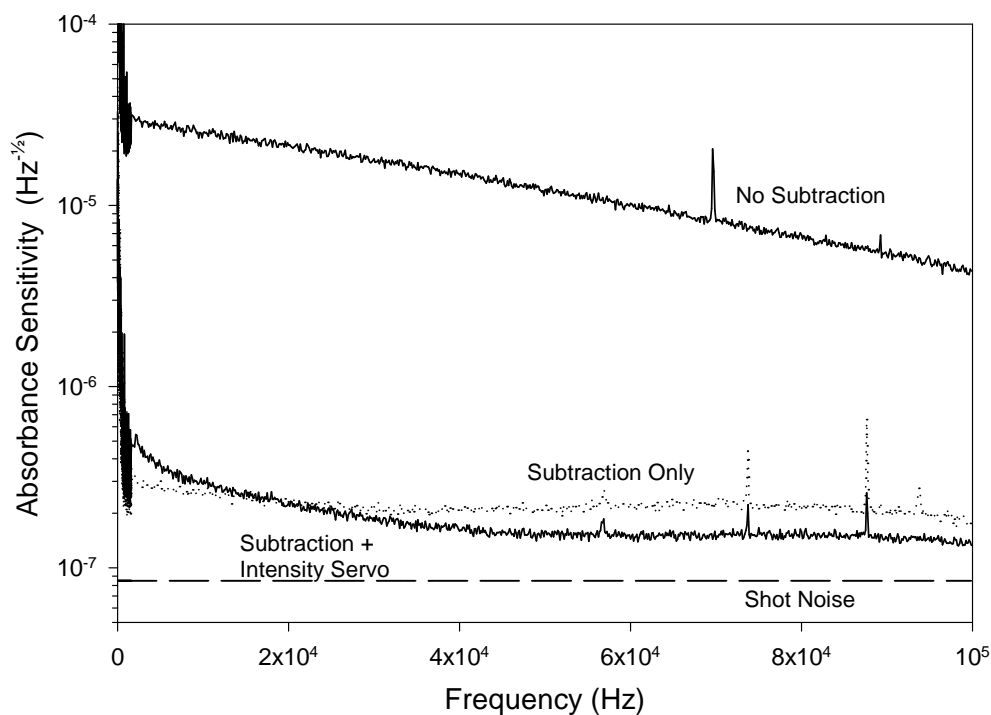


Figure 2-4. IR detection noise spectrum. The top trace shows the noise as viewed on a single detector. The intensity servo works to modulate the intensity of the Kr ion laser to cancel the noise on the reference InSb detector. The combination of this servo and signal subtraction puts our detection sensitivity to within a factor of two of the shot noise limit.

The subtracted signal is digitized and averaged with a 100 MHz digital oscilloscope. A typical data trace reflects approximately 250 averages. The averaged signal is transferred via a GPIB interface to a computer for storage and

analysis. The end result is an OH temporal profile with an absorption sensitivity of $2 \times 10^{-8} \text{ Hz}^{-1/2}$.

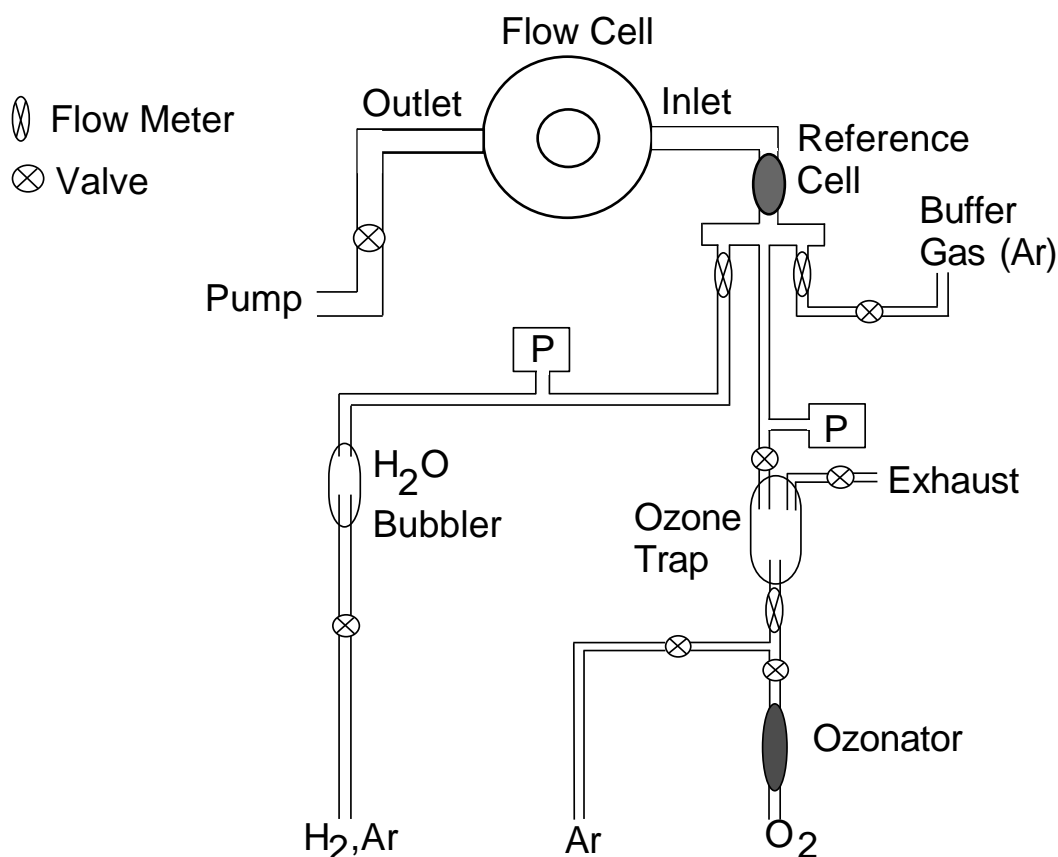


Figure 2-5. The gas handling system. Concentrations in the cell are proportional to their relative flow rates (equation 2.6), as measured by mass flow meters. Ozone is produced by an AC arc discharge (ozonator), and stored on silica gel at a temperature of $\sim 200\text{K}$. The absolute ozone concentration of the ozone is determined by 308nm absorption in the flow cell, and relative ozone concentration is measured by 254nm absorption in an 8.57 mm cell (reference cell). H_2O is added to the cell by flowing Ar or H_2 through a bubbler filled with H_2O . The fraction of H_2O present in the flow is determined by its vapor pressure at room temperature.

The various reactant and precursor gases are introduced into the flow cell by the gas handling system shown in figure 2-5. The concentrations are determined via their relative flow rates, which are measured by mass flow meters which are calibrated prior to the experiment by timing a pressure rise into a known volume. A

measured flow of Ar is passed through the ozone trap, where ozone is eluted into the Ar flow. A second gas flow into the flow cell is formed by passing Ar or H₂ gas through a porous frit immersed in a H₂O bubbler, which generates an H₂O concentration at the equilibrium vapor pressure, as shown in figure 2-6. At temperatures below 240K, however, we bypassed the H₂O bubbler and used a flow of pure H₂ to serve as the precursor gas. A third flow meter measures the flow of Ar buffer gas into the cell.

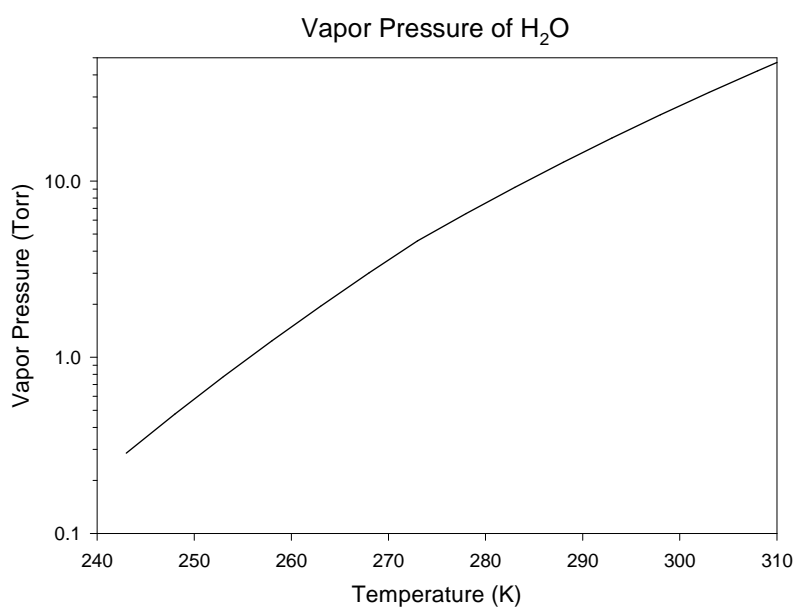


Figure 2-6. Vapor pressure of water as a function of temperature.

The partial pressure of each species in the cell is determined by the following equation:

$$P_i = \frac{f_i \chi_i}{\sum_i f_i} P_{\text{TOT}}, \quad (2.6)$$

where f_i is the flow rate as measured by the particual mass flow meter, χ_i is the fraction of the species present within the particual flow, and P_{TOT} is the total pressure in the flow cell as measured by a 100 Torr Baratron gauge.

Ozone is produced in an AC discharge from molecular oxygen (99.99%) and adsorbed in a pyrex cylinder filled with silica gel at approximately -110°C .^{8,9} Prior to entering the flow tube, the concentration of ozone is determined by absorption of the Hg emission line at 253.7 nm in a calibrated 8.56 mm transmission cell, based on the known absorption cross section¹⁰⁻¹² of $\sigma = 1.137 \times 10^{-17}\text{ cm}^2$. In addition, the absolute concentration of ozone is measured in situ via 308 nm UV absorption. Because of the important role the absolute concentration of ozone plays in the determination of the rate constant, it is of utmost importance that the measurement be accurate. For this reason, we utilize the *in situ* ozone concentration measurement to determine the absolute ozone density. In order to do this properly, we must take into account subtle experimental factors, such as the proper emission wavelengths of the XeCl excimer and the temperature dependence of the ozone cross section at 308 nm. The ozone UV cross section is calculated using a weighted average of the two XeCl emission lines (307.9 nm and 308.2 nm) with their proper 2:5 integrated intensity ratio.¹³ We also corrected the ozone cross section at these wavelengths for their temperature dependence, as shown in figure 2-7.^{14,15}

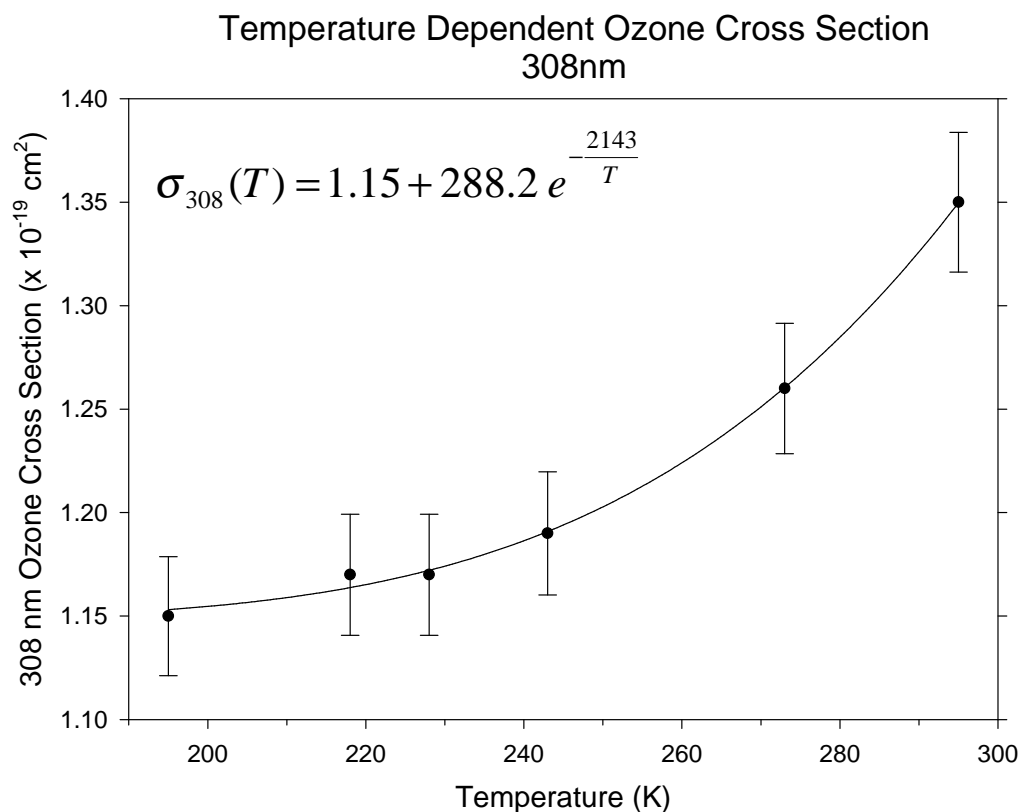


Figure 2-7. Temperature dependence of the ozone cross section^{14,15} at 308 nm. Each cross section is based on the XeCl emission lines at 307.9 and 308.2 nm, with a 2:5 integrated intensity ratio.

In order to properly interpolate the cross section between measured temperatures, the data is fit to an exponential form given by

$$\sigma_{308}(T) = A + B e^{-\frac{C}{T}}, \quad (2.7)$$

where $A = 1.15 \times 10^{-19} \text{ cm}^2$, $B = 288 \times 10^{-19} \text{ cm}^2$, and $C = 2143 \text{ K}$. This form is chosen to reflect a simple “Arrhenius-type” expression. That is, at any given temperature, the probability of absorption of 308nm light by an ozone molecule is given by $e^{-\frac{C}{T}}$. As T increases to infinity, σ_{308} becomes $A + B$, and as T decreases to zero, σ_{308} goes to A . A table of the 308 nm ozone UV cross sections as well as the

corresponding quantum yields for O(¹D) (Φ) at various temperatures appears in table 2-1.

Temperature (K)	$\sigma^{308}[\text{O}_3]$ (10^{-19}cm^2)	$\Phi^{308}[\text{O}_3]$ (%)
334	[1.62(8)]	[81]
314	[1.46(7)]	[81]
295	1.35(3)	81
287	1.31(3)	80
273	1.26(3)	76
266	1.24(3)	74
253	1.21(3)	68
250	1.20(3)	66
240	1.19(3)	60

Table 2-1. The temperature dependant cross section^{14,15} (σ) and quantum yield⁴ (Φ) for ozone at 308nm. The numbers in braces represent extrapolation from measured quantities.

2.3 The Temperature-Controlled Flow Cell

The temperature-controlled flow cell used for these experiments is shown in figure 2-3. The tube is made entirely of quartz, and consists of a gas inlet/outlet manifold, reaction chamber, and cooling jacket.

The reaction chamber is a tube 106 cm long, 2.5 cm in diameter, with a volume of 0.56 L. The ends of the chamber are made of IR grade, quartz optics, with a transmittance of >90% in both the IR and UV. Each end of the reaction chamber has a set of such optics, separated by an evacuated chamber. This evacuated chamber, positioned outside the cooling jacket, serves to protect the optics from condensation at low temperatures. Each optic is tilted at approximately 5° from normal to minimize interference effects due to reflections from the surface. The reaction chamber possesses three observation ports, allowing measurement of

parameters such as temperature and pressure. In addition, there are two ports, on either end of the cell, that allow cleaning of the interior surface of the optics.

Gas enters and leaves the reaction chamber through the gas inlet/outlet manifold. The gas inlet system runs the entire length of the tube, allowing fresh gas to flow into each area of the chamber. Offset from these inlet ports are the outlet ports, through which the gas is pumped away. The result is a net flow *across* the reaction chamber that serves to reduce concentration and temperature gradients of the reactants and products along the length of the cell. The rate of this flow is determined by the total rate of flow into and out of the tube, but under typical conditions, the reaction chamber is refreshed every 10 seconds.

The cooling jacket surrounds the gas inlet/outlet systems and the reaction chamber. The jacket contains a fluid, whose temperature is varied externally via a heat-exchanger apparatus. The fluid is circulated by a 32 L/min pump between the cooling jacket of the flow cell and a copper heat-exchanger coil, immersed in a constant temperature bath. At this pumping speed, the fluid in the cooling jacket is refreshed every 15 seconds.

The choice of fluids used in the heat-exchanger bath and the cooling jacket is dictated by the temperature that one wishes to achieve. It is imperative that the freezing point of the fluid used in the cooling jacket be lower than that of the heat-exchanger bath. Otherwise, freezing of the fluid might occur, causing damage to the flow tube. A table of various fluids and their freezing points are contained in table 2-2.

Fluid	Freezing Temperature (C)
Water	0
Ethanol	-115
Pentane	-130

Table 2-2. The freezing point for various fluids used to cool the cell.

2.4 The Questek Excimer Laser

Performance of the Questek 2000 series excimer laser is dependant on two factors: (1) gas purity, and (2) electrode conditions. Gas purity is a general concern, especially when switching the excimer from a chlorine-based mixture to a fluorine-based mixture. The Questek manual describes a procedure for successfully changing gas mixtures, but experience has shown that it is necessary to open the chamber and physically clean all surfaces. In addition, multiple fluorine passivation cycles must be performed before the laser operates reliably.

Electrode and discharge conditions play an important role in the operation of the laser. If proper safety precautions are taken, it is possible to view the discharge using a reasonably thick piece of plexi-glass (1" - 2" thick). However, if there is a non-lasing mix in the chamber, it is possible to view the discharge with a pair of lab safety glasses. During the discharge, one should see an even glow between the two electrodes. The discharge should be free of any sparks, or "lightning bolts", between the electrodes, which will eventually damage its surface. If these sparks are visible, it may indicate uneven spacings between the pre-ionization pins located on either side of the electrode assembly. The pre-ionization pin spacing is 0.040", which is much smaller than the 0.740" spacing of the electrodes. Hence, a small

electric discharge occurs between the pins, catalyzing the breakdown between the electrodes. These pre-ionization gaps increase over time, due to the harsh environments to which they are constantly exposed. When this occurs, it is necessary to readjust or replace the pins. Prolonged exposure to improper breakdown conditions will cause the electrodes to become pitted. Because the electrodes are made of solid nickel, they can be polished. However, one must take care to preserve the slight bow along the length of its surface.

2.5 The Kr Ion Laser

The Kr ion laser acts as a pump laser for the F-center laser. In order to insure reliable operation of the Kr ion laser, constant attention and care are required. In order to more fully understand the operation of the ion laser, a block diagram outlining the major components is included in figure 2-8.

In order to pump the F-Center laser properly, it is necessary to have at least one Watt of output power. This value of one Watt originates from the 800 mWatts needed to pump the F-Center laser plus an extra 20% to make up for loss from the intensity servo. If the Kr ion laser cannot achieve this power, the most likely cause is overpressure of Kr in the tube. As the pressure in the tube increases, the effective resistance of the tube increases. Therefore, for a given tube voltage, the current will decrease as the effective resistance increases. In order to recover the lost power, one must either increase the voltage or decrease the pressure. Increasing the voltage on the laser tube is achieved by adjusting the taps on the auto-transformer in the power supply. A table containing laser tube voltage and tap positions is shown in table 2-3.

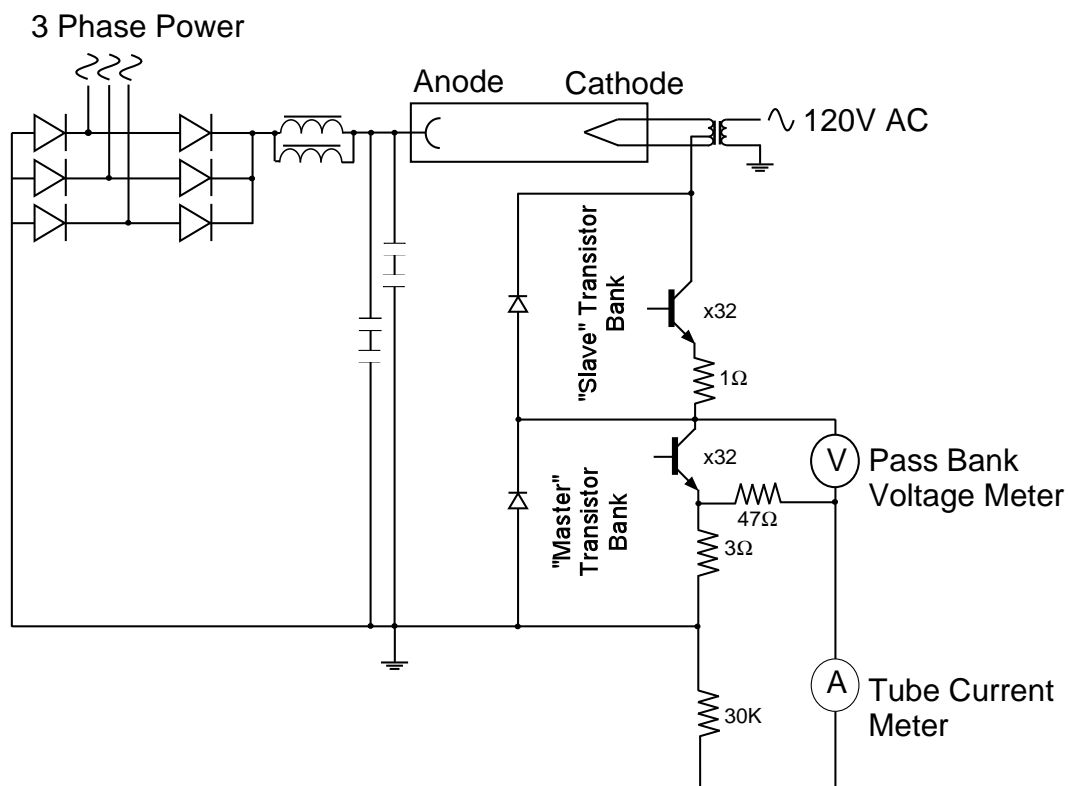


Figure 2-8. Block diagram of the Kr ion laser.

Tap Position (Primary lead = 9)	Tube Voltage (Volts)
1	435
2	460
3	485
4	510
5	540
6	560
7	575
8	600

Table 2-3. Kr ion laser tube voltage at various auto-transformer tap positions

The pressure of the laser tube can be measured via the Hastings TC gauge located near on the cathode end of the ballast reservoir. Unfortunately, we do not have a Hastings TC gauge reader. We have calibrated one of the ubiquitous Varian

801 TC gauge readers in the lab in order to read the actual pressure in the tube. This calibration curve is contained in figure 2-9. The optimum Kr pressure in the tube is 150 mTorr (180 mTorr as read by Varian 802 gauge). If the pressure in the tube is 50% greater than optimum, it is necessary to pump the laser tube down to its optimum pressure.

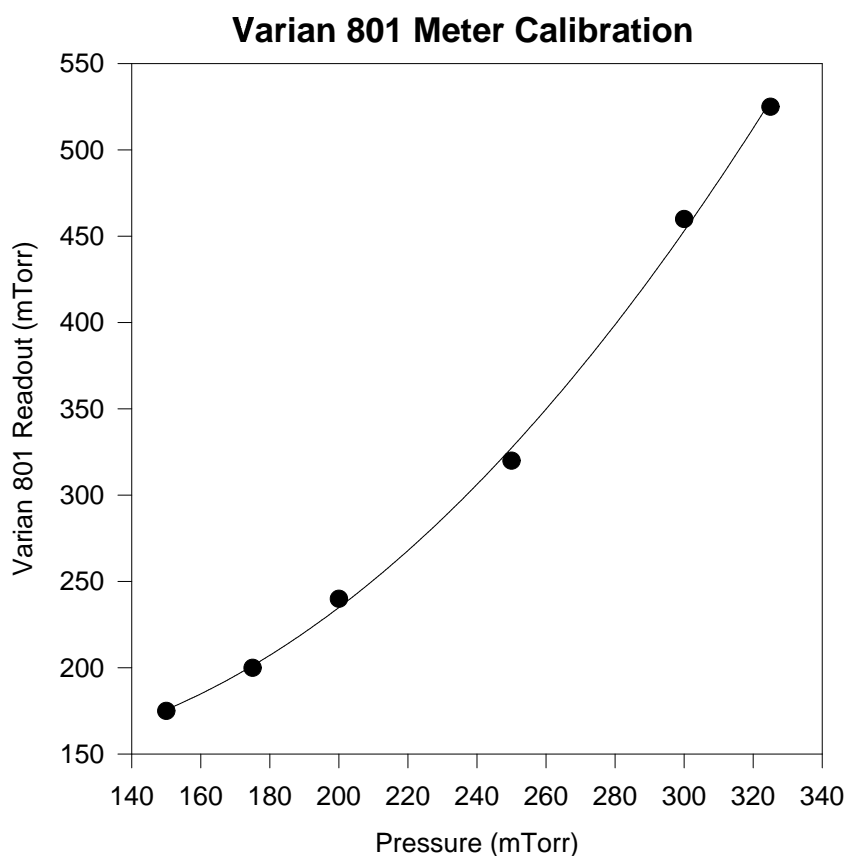


Figure 2-9. Calibration of the Varian 801 meter reading a Hastings TC gauge. Optimum tube pressure is 150 mTorr, which reads as approximately 180 mTorr on the Varian 801 gauge. The data above is fitted to a 2nd order polynomial with the following coefficients: $a[0] = 197.3$, $a[1] = -1.141$, $a[2] = 6.644 \times 10^{-3}$.

Pumping the laser tube is very risky, and great care must be taken to insure the purity of the Kr is not compromised. All tubing must be clean, and all joints must be vacuum tight. A liquid-nitrogen trapped, diffusion pump system works especially well. Due to the small orifice of the Nupro valve on the Kr ion laser tube, overloading the diffusion pump is not a concern. Typically, it takes approximately 20 minutes to reduce the pressure in the Kr laser tube by 50 mTorr.

The transistor bank serves to regulate the current through the laser tube by limiting the tube voltage. Because of the high currents (~40 Amps) and voltages (~500 V), the regulating transistors must work in parallel, dividing the voltage and current between them. The most common failure mode of the laser is the shorting of one or more transistors in the “Master” or “Slave” power transistor bank. When this occurs, it is necessary to find the “blown” transistor and replace it.

The test circuit for the “Master” transistor bank is shown in figure 2-10.

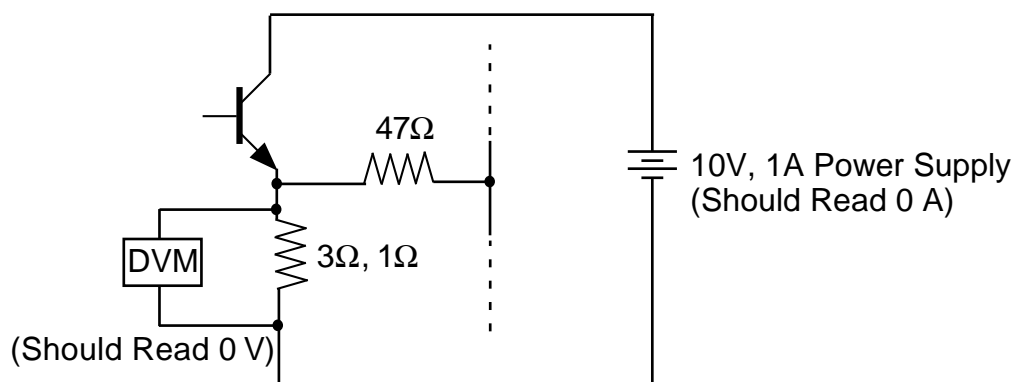


Figure 2-10. Test circuit for the “Master” and “Slave” transistor banks. When testing the “Slave” bank, it is also necessary to disconnect the driver transistor. A properly working transistor bank should sink very little current, and the voltage drop over the 3Ω (1Ω for “Slave”) should be negligible.

Using a ~1A current limiting power supply, connect the positive lead to the transistor's collector, and the ground lead to the 3 Ohm resistor. If the transistor is blown, the power supply current should read its limiting value, and the voltage drop over the 3 Ohm resistor should be the voltage difference between the leads. A properly working power transistor bank should sink very little current (~50 mA), and the voltage drop over the 3 Ohm resistor should be 0 Volts.

The procedure for testing the "Slave" transistor bank is very similar to the above procedure. However, it is necessary to first disconnect the small driver transistor (not shown in block diagram). If you do not disconnect this driver transistor, the "Slave" bank will sink current even if working properly. After disconnecting the driver transistor, the "Slave" transistor bank can be tested in the same manner as the "Master" transistor bank (see test circuit in figure 2-10).

References for Chapter 2

- 1 D. D. Nelson Jr, A. Schiffman, and D. J. Nesbitt, *J. Chem. Phys.* **93**, 7003 (1990).
- 2 A. Schiffman and D. J. Nesbitt, *J. Chem. Phys.* **95**, 2629 (1991).
- 3 A. Schiffman and D. J. Nesbitt, *J. Chem. Phys.* **100**, 2677 (1994).
- 4 W. B. DeMore, S. P. Sander, D. M. Golden, R. F. Hampson, M. J. Kurylo, C. J. Howard, A. R. Ravishankara, C. E. Kolb, and M. J. Molina, (Jet Propulsion Laboratory, Pasadena, California, 1994).
- 5 A. Schiffman, D. D. Nelson Jr., M. S. Robinson, and D. J. Nesbitt, *J. Phys. Chem.* **95**, 2629 (1991).
- 6 J. L. Hall and S. A. Lee, *Appl. Phys. Lett.* **29**, 367 (1976).
- 7 W. B. Chapman, , University of Colorado, Boulder, 1997.
- 8 E. Coleman, T. Siegrist, D. A. Mixon, P. L. Trevor, and D. J. Trevor, *J. Vac. Sci. Technol.* **A9**, 2408 (1991).
- 9 G. A. Cook, A. D. Kiffer, C. V. Klumpp, A. H. Malik, and L. A. Spence, *Ozone Chemistry and Technology* (American Chemical Society, Washington, 1959).
- 10 K. J. Mauersberger, D. Hanson, and J. Morton, *Geophys. Res. Lett.* **13**, 671 (1986).
- 11 A. G. Hearn, *Proc. Phys. Soc. London* **78**, 932 (1961).
- 12 G. Brasseur and S. Solomon, *Aeronomy of the Middle Atmosphere* (Reidel, Dordrecht, 1986).
- 13 G. Mount, *J. Geophys. Res.* **97**, 2427 (1992).
- 14 J. Brion, A. Chakir, D. Daumont, J. Malicet, and C. Parisse, *Chem. Phys. Lett.* **213**, 610 (1993).
- 15 D. Daumont, J. Brion, J. Charbonnier, and J. Malicet, *J. Atmos. Chem.* **15**, 145 (1992).